

Improved Accuracy of Diffusion MRI Tractography Using Topology-Informed Pruning (TIP)

Fang-Cheng Yeh M.D. Ph.D.^{1,2,*}, Sandip Panesar M.D.¹, Jessica Barrios M.D.¹, David Fernandes M.D.¹,
Kumar Abhinav M.D.³, Antonio Meola M.D. Ph.D.³, Juan C. Fernandez-Miranda M.D.³

¹Department of Neurological Surgery, University of Pittsburgh Medical Center, Pittsburgh, Pennsylvania,
USA

²Department of Bioengineering, University of Pittsburgh Medical Center, Pittsburgh, Pennsylvania, USA

³Department of Neurosurgery, Stanford University School of Medicine, San Jose, California, USA

*Correspondence to:

Fang-Cheng Yeh, M.D. Ph.D.

Department of Neurological Surgery,

Department of Bioengineering,

University of Pittsburgh, Pittsburgh, Pennsylvania

Email: frank.yeh@pitt.edu

1 **Abstract**

2 Diffusion MRI fiber tracking provides a non-invasive method for mapping the trajectories of human brain
3 connections, but its false connection problem has been a major challenge. This study introduces
4 topology-informed pruning (TIP), a method that improves the tractography of a target fiber bundle using
5 its own topology information. TIP identifies singular tracts and eliminates them to improve the tracking
6 accuracy. This method was applied to a tractography study with diffusion MRI data collected using two
7 different diffusion sampling schemes (single-shell and grid). The accuracy of the tractography was
8 evaluated by a team of 6 neuroanatomists in a blinded setting to examine whether TIP could improve the
9 accuracy of tractography. The results showed that TIP achieved an average accuracy improvement of
10 11.93% in the single-shell scheme and 3.47% in the grid scheme. The improvement is significantly
11 different from a random pruning (p -value < 0.001). The diagnostic agreement between TIP and
12 neuroanatomists was comparable to the agreement between neuroanatomists. The proposed TIP
13 algorithm can be used to automatically clean up noisy fibers in deterministic tractography, with a
14 potential to confirm the existence of a fiber connection in basic neuroanatomical studies or clinical
15 neurosurgical planning.

16 **Key words:** deterministic fiber tracking, tractography, topology, structural connectome, diffusion MRI

1 **Introduction**

2 Diffusion MRI fiber tracking provides a non-invasive way of mapping macroscopic connections in the
3 human brain, but validation of tractography results remains a challenge [1, 2]. A large-scale study
4 examined 96 methods submitted from 20 research groups, showing that the accuracy of tractography
5 quantified by the percentage of valid connections ranged from 3.75% to 92% due to differences in
6 reconstruction methods and algorithms [3]. Proposed strategies to improve fiber tracking included
7 motion correction, eddy current correction, and tractography clustering. Nonetheless, even if an optimal
8 strategy demonstrated improvement, there were still a substantial amount of false connections. With an
9 ultimate goal of studying the human connectome, tractography cannot advance unless results can be
10 consistently and reliably validated [4].

11 Our recent HCP-842 tractography study provided insights into false connections generated by
12 deterministic tractography approaches [5]. By using human neuroanatomists to analyze the
13 neuroanatomical labels and eliminate false continuities, the study identified two major reasons for false
14 connections: premature termination of tracking algorithms and false continuations. Premature
15 terminations can be addressed by using a white matter mask, which allows for automatic checking of the
16 fiber trajectory endpoints. False endpoints are rejected for better accuracy. Studies previously used
17 demarcation between white and gray matter boundaries, derived from T1-weighted images as an

1 tract-termination benchmark [6]. False tracts were determined as those prematurely terminating in white
2 rather than gray matter, whilst real tracts were defined as those which terminated in gray matter, as
3 determined by the overlap of T1 and diffusion-weighted images. False continuities, on the other hand,
4 cannot be easily addressed using structural images or diffusion data. This is due to the limitation of
5 diffusion MRI techniques in resolving the exact configuration of crossing fibers such as bending, fanning,
6 or interdigitating [7]. Diffusion signals cannot alone differentiate these configurations within the voxel
7 space. Until now, *a priori* knowledge of white matter anatomy was necessary to validate tractography
8 results. Our recent atlas study [5] demonstrated an interesting pattern, however, that potentially enables
9 automated differentiation between false and real tracts: After separating whole-brain trajectories into
10 clusters based on their neighboring distance, clusters with fewer neighboring tracts were more likely to
11 contain false connections. Neighboring tracts share similar trajectories, with close-proximity endpoints.
12 This finding suggests that a track with few neighboring tracts has a high likelihood of being a false
13 continuity. One potential explanation of this phenomenon is that the false tracts arise between the
14 overlapping boundaries of two real, adjacent fiber bundles. Since this overlapping boundary only forms a
15 touching surface or line between two fiber pathways, it will only allow for a limited number of trajectories
16 to pass through. Moreover, it is known that errors of fiber tracking will accumulate during the tracking
17 process [8]. As a result, the trajectories that pass through the overlapping boundaries tend to have very

1 diverse propagation routes due to the perturbation around the boundaries. These two unique conditions
2 combined will greatly reduce the chance of a false tract to find a neighboring fiber trajectory. This
3 observation thus brings forth our *singular tract hypothesis*—a singular tract (i.e. a trajectory with no
4 neighboring tract) has a higher likelihood of being a false connection. This hypothesis further inspired
5 our topology-informed pruning (TIP) algorithm, which uses the topology of tractography itself to identify
6 candidate false connections for removal. It was realized by first constructing a 3D tract density histogram
7 to single out voxels with only one track passing through them, then subsequently eliminating those
8 singular tracts to improve the accuracy. We examined the performance of TIP using data from our
9 previous study. We tracked the arcuate fasciculus using a single region of interest (ROI) placed around
10 the angular gyrus. The TIP tractography result was then independently scrutinized by 6 neuroanatomists
11 to assess whether TIP could reduce the percentage of false connections.

12 **Materials and Methods**

13 *The TIP Algorithm*

14 The TIP algorithm is illustrated in Fig.1. The input data are a set of trajectories obtained from the
15 tractography of a target fiber bundle (Fig.1a). The tractography of a fiber bundle can be obtained from a
16 region-of-interest or any track selection approach. The number of trajectories should be high enough to

1 produce a 3D histogram (yellow density map in Fig. 1b). A tract may pass through the same voxel more
2 than one time but it only be counted once in the histogram. The second step is to identify voxels with
3 track density equal to one (red density map in Fig. 1b). These voxels are nearby white matter regions
4 where singular tracts “go astray” via an overlapping boundary. These tracts are identified and excluded
5 from the bundle (Fig. 1c) to produce a pruned tractogram (Fig. 1d). The whole process can be repeated
6 until no more singular tracts are found. The computation complexity of TIP is $O(N)$, where N is the
7 number of trajectories.

8 *TIP applied to the arcuate fasciculus tractography*

9 We applied TIP to existing data from our previous tractography study [9] to examine whether TIP can
10 improve the accuracy of tractography. The data were originally acquired from a normal subject scanned
11 in a 3T Siemens Tim Trio MRI scanner, using a twice-refocused echo planar imaging (EPI) diffusion
12 pulse sequence. Both a 253-direction single-shell scheme and a 203-direction grid scheme were
13 acquired. For the 253-direction single shell scheme, the diffusion parameters were TR/TE = 7200
14 ms/133 ms, b-value = 4,000 s/mm², and the scanning time was approximately 30 minutes. For the
15 203-direction grid scheme, the diffusion parameters were TR/TE = 7200 ms/144 ms, the maximum
16 b-value = 4,000 s/mm², and the scanning time was approximately 25 minutes. The shell and grid

1 sampling schemes shared the same spatial parameters: the field of view was 240 mm × 240 mm, the
2 matrix size was 96 × 96, and the slice thickness was 2.5 mm. A total of 40 slices were collected.

3 DSI Studio (<http://dsi-studio.labsolver.org>) was used to track the arcuate fasciculus using a method
4 identical to the original study [9]. To summarize, the generalized q-sampling imaging reconstruction was
5 applied to both sampling schemes with a diffusion sampling length ratio of 1.25. A 14-mm radius
6 spherical ROI was placed at the angular gyrus, and tracts passing the ROI connecting temporal with
7 frontal regions were selected. The tractography was generated using an angular threshold of 60 degrees
8 and a step size of 1.25 mm. Whole-brain seeding was conducted until a total of 2,000 fiber tracts were
9 generated from the ROI.

10 6 neuroanatomists (S.P., D.F., J.B., J.F., K.A., A.M.) independently examined the tractography to
11 identify false tracts. The examination was conducted by a blinded setting. They were instructed to
12 remove false tracts from the tractography and were unaware of the TIP algorithm, nor did they have
13 access to the TIP-processed tractography, or teach others results. The accuracy of the tractography was
14 then quantified using the following formula:

$$15 \quad \frac{N-a}{N} \times 100\% \quad (1)$$

1 where N is the total number of tracts, and a is the number of tracts identified as false connections. The
2 accuracy of the TIP-processed tractography was calculated using the same formula. N represents
3 non-singular tracts, and a is the number of non-singular false tracts as identified by the neuroanatomists.
4 TIP could also be viewed as an observer, and we further quantified the diagnostic agreement between
5 TIP and any of the neuroanatomists by the following formula:

$$6 \quad \frac{a+b}{N} \times 100\% \quad (2)$$

7 Where a is the number of positive agreements quantified by the number of singular, false tracts
8 simultaneously identified by TIP and the neuroanatomists. b is the number of positive agreements
9 quantified by TIP as non-singular and “not-false” by the neuroanatomists. N is the number of total tracts
10 evaluated. 6 diagnostic agreements were calculated between TIP and any of the 6 neuroanatomists.
11 The diagnostic agreements between the neuroanatomists were also calculated for a comparison.

12 **Results**

13 Figure 2a shows the tractogram of arcuate fasciculus before and after being pruned by the TIP algorithm.
14 The tractography generated using the angular gyrus ROI shows “noisy” fibers (Fig. 2a), especially using
15 the single-shell scheme. The tractography using the grid sampling scheme appears to be cleaner, but
16 deviant trajectories are still visible. TIP effectively removes noisy fiber while retaining the main topology

1 structure. The improvement is particularly striking in the single-shell scheme. The pruned tractography
2 appears to be consistent with the microdissection results (Fig. 2b, adopted from [9]).

3 *Accuracy of TIP-processed tractography*

4 The accuracy of tractography before and after TIP is quantified in Fig.3. The tractography from a
5 single-shell scheme is shown in Fig. 3a, whereas the tractography from the grid scheme is shown in Fig.
6 3b. A total of 6 different evaluations were conducted independently by the 6 neuroanatomists. The lines
7 connect evaluations from the same neuroanatomists. In both Fig. 3a and 3b, all evaluations
8 unanimously showed improved accuracy after TIP was applied to the arcuate fasciculus tractography.
9 The average improvement in the single-shell scheme was 11.93%, whereas the average improvement
10 in the grid scheme was 3.47%. Improvement is most obvious in the single-shell dataset. The lower
11 improvement in the grid scheme could be due to its lower sensitivity for demonstrating branching fibers,
12 as shown in the original tractography before pruning.

13 We further compare the performance of TIP with random pruning. Since random pruning (e.g. random
14 elimination of an arbitrary number of tracts) will result in an equal opportunity between increased
15 accuracy and decreased accuracy, the chance that 6 evaluations unanimously present improved
16 accuracy in random pruning is thus $1/2^6=0.015625$ (follows a binomial distribution), and the probability of

1 this happening on both single-shell and grid datasets is thus $(1/2^6)^2 = 0.00024414062$. Therefore, for a
2 null hypothesis that TIP is no different from random pruning, the p-value will be smaller than 0.001
3 based on this frequentist hypothesis-testing framework, and thus we can conclude that TIP is
4 significantly different from random pruning.

5 *Diagnostic agreement between TIP and neuroanatomists*

6 Figure 4 compares the tractograms produced when false tracts are removed by a representative
7 neuroanatomist, compared with the same tracts pruned by TIP. The neuroanatomist chosen here had
8 the highest diagnostic agreement with the other 5 neuroanatomists and thus can be viewed as the
9 representative neuroanatomist of the group. In both the single-shell and grid schemes, the
10 TIP-processed tractography was highly consistent with the neuroanatomist-pruned tractography, though
11 differences can still be observed at minor branches.

12 We further evaluated the agreement of TIP with other neuroanatomists. Further quantification using
13 diagnostic agreement showed that the averaged diagnostic agreement between TIP and 6
14 neuroanatomists was 77.33% with the single-shell scheme and 77.73% with the grid scheme. In
15 comparison, the averaged diagnostic agreement between neuroanatomists was $77.46\% \pm 1.62\%$
16 (standard error) with the single-shell scheme and $75.80\% \pm 2.14\%$ with the grid scheme. The agreement

1 between TIP and neuroanatomists was within the standard error of the mean agreement between the
2 neuroanatomists. With the grid scheme, the average agreement between TIP and neuroanatomists was
3 even slightly higher than the average between the 6 neuroanatomists. We can conclude that the
4 agreement between TIP and neuroanatomists was comparable to the agreement within
5 neuroanatomists.

6 **Discussion**

7 Here we show that the topology of a tractography can be used to prune the tractography to achieve a
8 better accuracy. The TIP algorithm reduced the percentage of false tracts by 11.93% in single-shell
9 scheme and 3.47% in the grid scheme. The performance difference can be explained by the fact that the
10 single-shell tractography in our study captured more branching fibers, and the trajectories appeared to
11 be “nosier”. The pruning effect was thus more dramatic in such a high sensitivity setting. Although the
12 improvement with the grid scheme is limited, the evaluations by all 6 neuroanatomists unanimously
13 indicated improved accuracy after pruning. Moreover, the agreement of TIP with neuroanatomists was
14 comparable to the agreement between the neuroanatomists alone. This suggests that TIP can replace a
15 substantial part of the evaluation work done by neuroanatomists to scrutinize tractography.

1 TIP appears to be a unique tract validation method using only the relationship between individual tracts
2 within the tractogram as a benchmark. Its theoretical basis differs from other post-processing methods
3 which rely on diffusion MRI signals, T1W, or other imaging modalities to remove false connections [6,
4 10]. While the T1W or other imaging modalities can be used to improve the accuracy, using them to
5 capture false connections may introduce additional problems. For example, signal intensity in the T1W
6 images can be inhomogeneous, and segmenting white matter regions from T1W adds further complexity.
7 Using diffusion MRI signals as the prior may also present pitfalls of signal-distortion and artifacts in DWI.
8 These methods view each track as an independent target to be evaluated and do not use topological
9 information of the entire tract to eliminate false connections. The unique theoretical basis of TIP allows it
10 to potentially complement other anatomical-prior methods to improve tracking accuracy.

11 The computation time for TIP in our study was negligible in DSI Studio relative to the time taken for 3D
12 tractographic visualization. TIP only has linear complexity proportional to tract count (i.e. $O(N)$) and can
13 be readily applied to tractography with any number of trajectories. In comparison, a typical tract
14 clustering algorithm would require $O(N^2)$, which has limited capability for application to large fiber-count
15 bundles.

16 There are still limitations with TIP. We cannot rule out the possibility that a singular tract identified by TIP
17 is a real connection. This adverse result occurs if a small branch of a fiber bundles receives only limited

1 seeding points due to its small size. Insufficient seeding can result in limited numbers of neighboring
2 fibers, resulting in a valid connection being eliminated by TIP. The removal of these tracts results in
3 reduced sensitivity of tractography to capture small fiber pathways or branches. This means the
4 accuracy improvement from TIP comes with a trade-off for sensitivity to small branching fibers.
5 Moreover, applying TIP to whole brain tractography may not be an ideal utilization. The low-density
6 voxels of a fiber bundle can be occupied by nearby pathways, making the detection of singular tracts
7 difficult for TIP. A more sophisticated topology algorithm computing the distance between pair-wise
8 tracts for identification of singular tracts may be more appropriate. Nevertheless, the current TIP
9 algorithm is more suitable for tractography of a single bundle population versus whole-brain seeding.

10 Changing parameter settings for the TIP algorithm could expand its potential applications. For example,
11 the threshold for defining low-density voxels can be adjusted to adapt to a different seeding density. A
12 high threshold will yield highly confirmative results to justify existence of a fiber pathway. As more and
13 more fiber tracking studies have been proposed to discover human brain pathways and their
14 segmentations [11-14], TIP can strengthen the results by boosting the accuracy of tractography. The
15 number of recursive iterations can be limited to a small number to allow for different pruning effects. For
16 studies correlating structural connectivity with neuropsychological measures, a single iteration of TIP
17 can complement group connectometry analysis to achieve better false discovery rates. In neurosurgical

1 applications, TIP can assist mapping of peri-tumoral pathways to help neurosurgeons organize a
2 detailed surgical plan.

3

4 In conclusion, the topology information from a fiber bundle can be used to identify possible false
5 connections in order to achieve better anatomical validity. The TIP algorithm can be a useful tool to be
6 integrated with deterministic fiber tracking for mapping human brain connections.

7

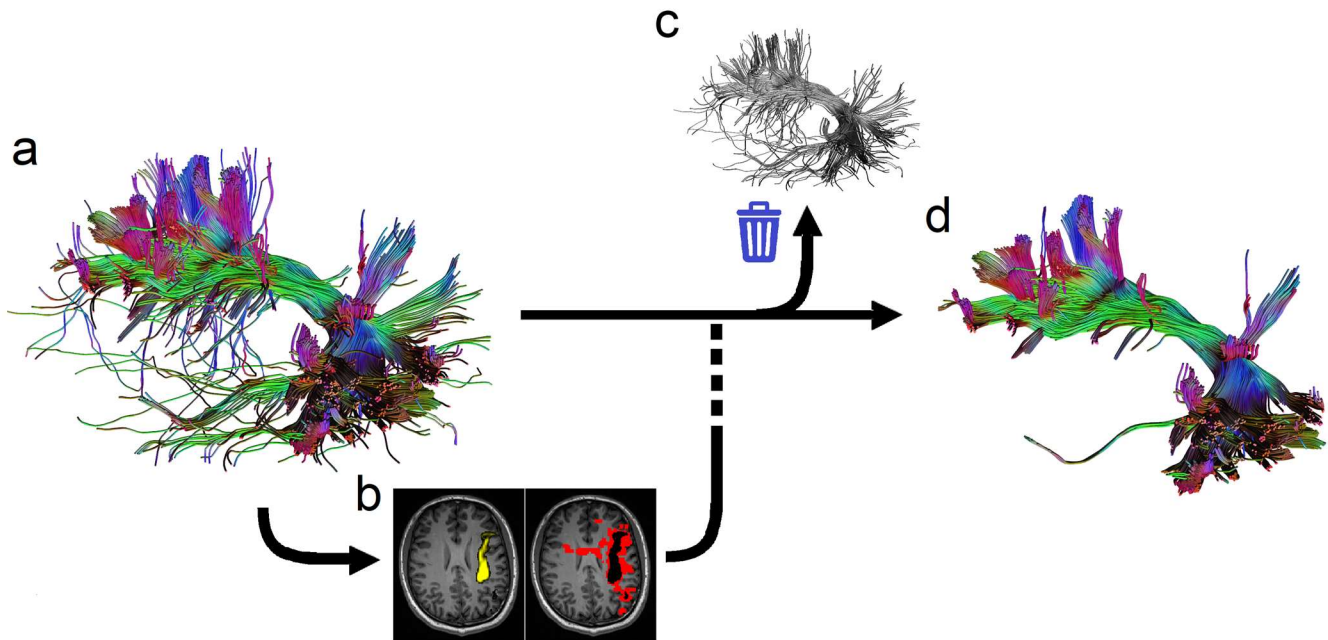
8 **References**

- 9 1. Reveley C, Seth AK, Pierpaoli C, Silva AC, Yu D, Saunders RC et al. Superficial white matter fiber
10 systems impede detection of long-range cortical connections in diffusion MR tractography. *Proc Natl*
11 *Acad Sci U S A*. 2015;112(21):E2820-8. doi:10.1073/pnas.1418198112.
- 12 2. Thomas C, Ye FQ, Irfanoglu MO, Modi P, Saleem KS, Leopold DA et al. Anatomical accuracy of
13 brain connections derived from diffusion MRI tractography is inherently limited. *Proc Natl Acad Sci U*
14 *S A*. 2014;111(46):16574-9. doi:10.1073/pnas.1405672111
15 1405672111 [pii].
- 16 3. Maier-Hein KH, Neher PF, Houde JC, Cote MA, Garyfallidis E, Zhong J et al. The challenge of
17 mapping the human connectome based on diffusion tractography. *Nat Commun*. 2017;8(1):1349.
18 doi:10.1038/s41467-017-01285-x.
- 19 4. Jbabdi S, Sotiropoulos SN, Haber SN, Van Essen DC, Behrens TE. Measuring macroscopic brain
20 connections in vivo. *Nat Neurosci*. 2015;18(11):1546-55. doi:10.1038/nn.4134.
- 21 5. Yeh FC, Panesar S, Fernandes D, Meola A, Yoshino M, Fernandez-Miranda JC et al.
22 Population-averaged atlas of the macroscale human structural connectome and its network topology.
23 *Neuroimage*. 2018;178:57-68. doi:10.1016/j.neuroimage.2018.05.027.

- 1 6. Smith RE, Tournier JD, Calamante F, Connelly A. Anatomically-constrained tractography: improved
2 diffusion MRI streamlines tractography through effective use of anatomical information. *Neuroimage*.
3 2012;62(3):1924-38. doi:10.1016/j.neuroimage.2012.06.005.
- 4 7. Tournier JD, Mori S, Leemans A. Diffusion tensor imaging and beyond. *Magn Reson Med*.
5 2011;65(6):1532-56. doi:10.1002/mrm.22924.
- 6 8. Basser PJ, Pajevic S, Pierpaoli C, Duda J, Aldroubi A. In vivo fiber tractography using DT-MRI data.
7 *Magn Reson Med*. 2000;44(4):625-32.
8 doi:10.1002/1522-2594(200010)44:4<625::AID-MRM17>3.0.CO;2-O [pii].
- 9 9. Yeh FC, Verstynen TD, Wang Y, Fernandez-Miranda JC, Tseng WY. Deterministic diffusion fiber
10 tracking improved by quantitative anisotropy. *PLoS ONE*. 2013;8(11):e80713.
11 doi:10.1371/journal.pone.0080713
- 12 PONE-D-13-26801 [pii].
- 13 10. Pestilli F, Yeatman JD, Rokem A, Kay KN, Wandell BA. Evaluation and statistical inference for
14 human connectomes. *Nat Methods*. 2014;11(10):1058-63. doi:10.1038/nmeth.3098.
- 15 11. Modo M, Hitchens TK, Liu JR, Richardson RM. Detection of aberrant hippocampal mossy fiber
16 connections: Ex vivo mesoscale diffusion MRI and microtractography with histological validation in a
17 patient with uncontrolled temporal lobe epilepsy. *Hum Brain Mapp*. 2016;37(2):780-95.
18 doi:10.1002/hbm.23066.
- 19 12. Meola A, Comert A, Yeh FC, Sivakanthan S, Fernandez-Miranda JC. The nondecussating pathway
20 of the dentatorubrothalamic tract in humans: human connectome-based tractographic study and
21 microdissection validation. *J Neurosurg*. 2016;124(5):1406-12. doi:10.3171/2015.4.JNS142741.
- 22 13. Meola A, Comert A, Yeh FC, Stefaneanu L, Fernandez-Miranda JC. The controversial existence of
23 the human superior fronto-occipital fasciculus: Connectome-based tractographic study with
24 microdissection validation. *Hum Brain Mapp*. 2015;36(12):4964-71. doi:10.1002/hbm.22990.
- 25 14. Yeatman JD, Weiner KS, Pestilli F, Rokem A, Mezer A, Wandell BA. The vertical occipital
26 fasciculus: a century of controversy resolved by in vivo measurements. *Proc Natl Acad Sci U S A*.
27 2014;111(48):E5214-23. doi:10.1073/pnas.1418503111.

28

29



1

2 Fig. 1 The topology-informed pruning (TIP) algorithm. (a) the input tractography of a target fiber bundle

3 is generated using adequate density of seedings. (b) the tractography is used to compute the density

4 map (yellow color) for identifying voxels with low track density (red color). (c) Tracts passing low density

5 voxels are eliminated from the tractography. (d) The resulting tractography from the TIP algorithm

6 eliminates singular tracts that are likely to be false connections.

7

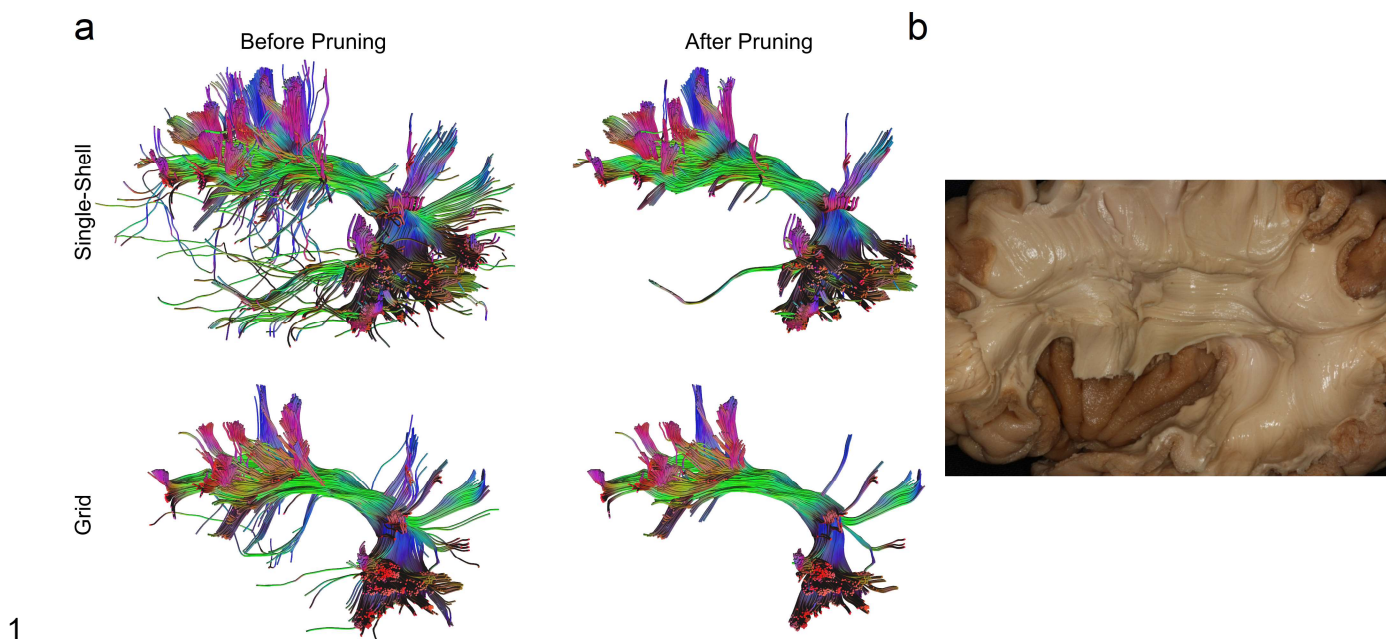
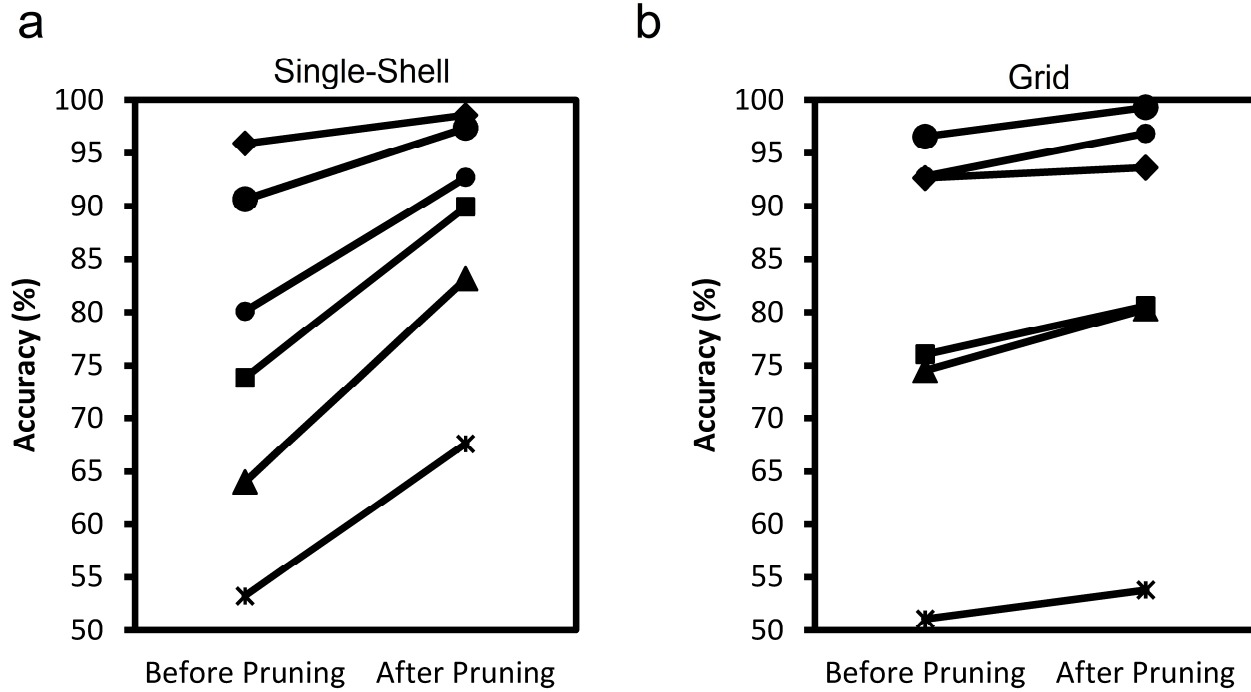


Fig. 2 (a) The arcuate fasciculus tractography after topology-informed pruning shows a coherent architecture with reduced noisy fibers. (d) Cadaver dissection of the nearby structures show consistent structure (adapted from [9]).



1

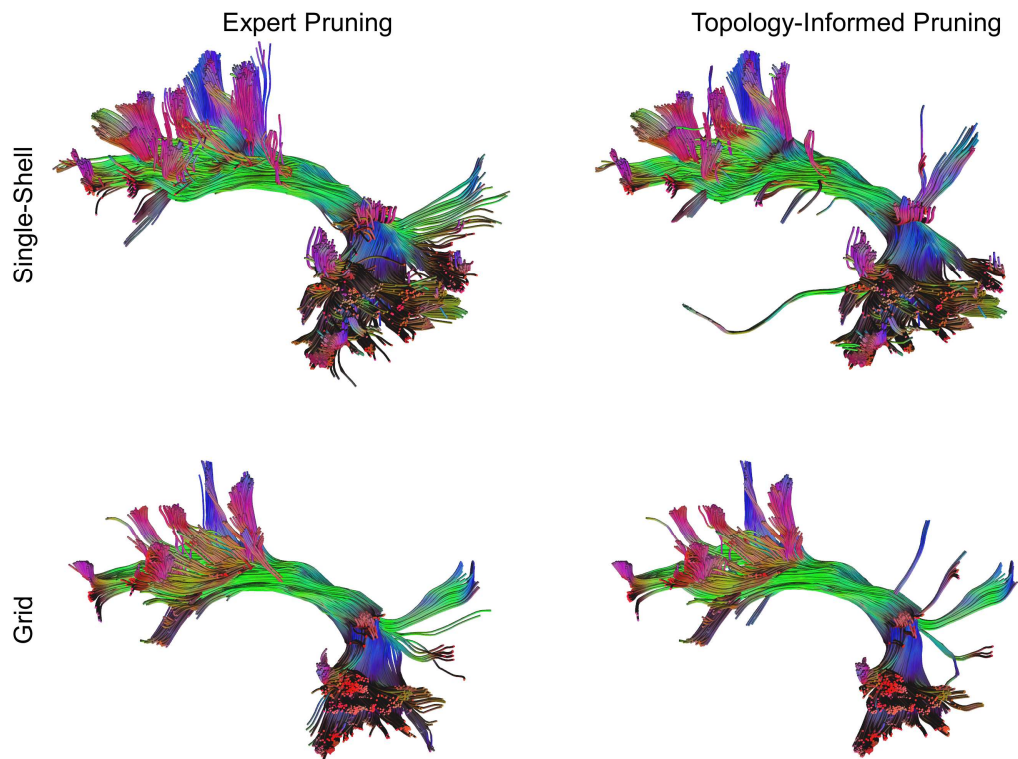
2 Fig. 3 Line plots showing the accuracy of tractography before and after pruning in (a) single-shell data

3 and (b) grid data. The line connects the two evaluations conducted by the same neuroanatomists. All

4 evaluations show increased accuracy after pruning. The improvement is most prominent in the single

5 shell dataset.

6



1

- 2 Fig. 4 Tractography pruned by a representative neuroanatomist compared with tractography pruned by
- 3 TIP. Although minor differences can still be found, the overall results show remarkable consistency in
- 4 the main structures and major branches.